



# Dinuclear Co(II)-Muconate Complex Displaying Distorted-Trigonal Prismatic Geometry, 2D Supramolecular Array and Weak Antiferromagnetism

Jonathan Jaramillo-García<sup>1</sup> · Raúl A. Morales-Luckie<sup>2</sup> · Diego Martínez-Otero<sup>2</sup> · Víctor Sánchez-Mendieta<sup>2</sup> · Roberto Escudero<sup>3</sup> · Francisco Morales<sup>3</sup>

Received: 11 May 2021 / Accepted: 24 September 2021

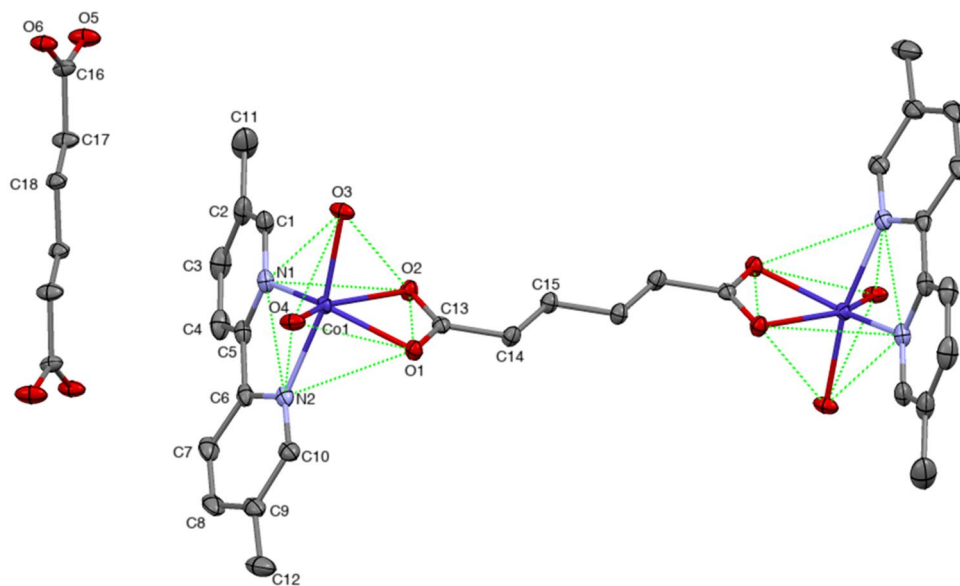
© The Author(s), under exclusive licence to Springer Science+Business Media, LLC, part of Springer Nature 2021

## Abstract

Dinuclear complex  $[\text{Co}_2(\text{H}_2\text{O})_4(\text{dmb})_2(\text{muc})][\text{muc}]$  (**1**) (muc = muconate; dmb = 5,5'-dimethyl-2,2'-bipyridine), was obtained by self-assembly solution reaction, under ambient conditions, and it was structurally characterized by elemental analysis, IR spectroscopy and single crystal X-ray diffraction. The complex **1** crystallizes in the monoclinic system in the  $C2/c$  space group. Noticeably, the six-coordinated Co(II) centers display a distorted-trigonal prismatic configuration. This uncommon coordination geometry is attained due to the hydrogen bonding interactions of the crystalline structure of **1**, yielding thus a 2D supramolecular array. Magnetic properties measurements reveal that metaprism **1** exhibits weak antiferromagnetic ordering with  $\theta_{(C-W)} = -14.4$  K and an  $E_2 = 0.032$   $\text{cm}^{-1}$  accordingly to Curie–Weiss model and Rueff phenomenological approach, respectively.

## Graphic Abstract

Influence of the 2D supramolecular array in the distorted trigonal prismatic geometry of a dinuclear Co(II)-muconate complex exhibiting weak antiferromagnetic exchange.



**Keywords** Dinuclear Co complex · Trigonal prismatic · Metaprism · Antiferromagnetism · Muconate

Extended author information available on the last page of the article

Published online: 07 October 2021

## Introduction

Hexa-coordinated d-block metal complexes continue to be dominated by octahedral geometries. Metaprisms ( $D_3$  symmetry) are intermediate geometries which can be formed when an octahedral coordination sphere (Oh symmetry) transforms into a trigonal prismatic geometry ( $D_{3h}$  symmetry) [1]. It has been reported that complexes getting metal ions with  $d^0$ ,  $d^1$ ,  $d^2$ ,  $d^5$  or  $d^{10}$  electron configurations are known to have an electronic predilection for the trigonal prismatic geometry [2]. It has also been proved that the bite angle and the electron configuration influence the coordination sphere of tris(chelate) complexes to move off from the octahedral geometry to a trigonal prismatic one [3]. Several metal complexes with trigonal prismatic geometry have been obtained with the use of non-innocent multi-chelating ligands and also by ligand design [4]. Nonetheless, in fewer cases, this geometry has been revealed in complexes using innocent bidentate ligands, and yet in complexes with monodentate ligands [5]. We have previously reported two complexes of Co(II) and Zn(II) [6] and one Mn(II)-muconate coordination polymer [7] where the metal ions possess a distorted-trigonal prismatic coordination sphere; the most important finding in this research has been, in addition to the factors above mentioned, the influence of the supramolecular structure in the formation of these metaprisms. There is also one more example reported in literature about metaprism complexes with innocent ligands, showing a Mn(II) coordination polymer having trigonal prismatic geometry [8]. Consequently, mixed ligands distorted-trigonal prismatic complexes of cobalt, using innocent ligands, can be still considered as unusual. Besides our reported Mn(II)-muconate polymer, *trans,trans*-muconate has also been used as a bridging ligand in Ni, Co, Cu and Zn coordination polymers [9–12], Mo dinuclear complexes [13] and a Pt macrocycle [14]. Additionally, there are also several interesting articles related to coordination polymers bearing the muc, or muco, as a bridging ligand.  $\{[Zn(\mu_1\text{-muco})(4\text{bpdh})(\text{H}_2\text{O})]\cdot\text{H}_2\text{O}\}$  and  $\{[Zn_2(\mu_3\text{-muco})_2(\mu\text{-3bpdb})_2(\text{H}_2\text{O})]\cdot 6\text{H}_2\text{O}\}_n$  (muco = *trans,trans*-muconate dianion, 4bpdh = 2,5-bis(4-pyridyl)-3,4-diaza-2,4-hexadiene and 3bpdb = 1,4-bis(3-pyridyl)-2,3-diaza-1,3-butadiene) were synthesized at room temperature [15]. These Zn(II) polymers, which are 1D and 3D, respectively, were studied as heterogeneous catalysts in the Knoevenagel reaction, and also their photoluminescent properties were evaluated. Moreover,  $[\text{Cu}_2(\text{muco})_2(4\text{-clpy})_2]$ ,  $[\text{Cu}_2(\text{muco})_2(4\text{-brpy})_2]$  ( $\text{H}_2\text{muco}$  = *trans,trans*-muconic acid; 4-clpy = 4-chloropyridine and

4-brpy = 4-bromopyridine) were synthesized along to other two Zn(II) coordination polymers, all having a 2D sheet structure [16]. Halogen-halogen supramolecular interactions were found in these two Cu(II) polymers, which had an important contribution in the  $\text{CO}_2$  sorption properties of these complexes. More recently,  $[\{\text{Cu}(\text{muco})(\text{bpa})(2\text{H}_2\text{O})\}\cdot 2\text{H}_2\text{O}]_n$  and  $[\{\text{Cu}(\text{muco})(4\text{bpdp})\}\cdot 2\text{DMF}\cdot\text{H}_2\text{O}]_n$  (4bpdp = 1,4-bis(4-pyridyl)-2,3-diaza-1,3-butadiene, bpa = 1,2-bis(4-pyridyl)ethane and muco = *trans,trans*-muconate dianion) were synthesized and characterized; the inhibitory action of both complexes against the *Staphylococcus aureus* biofilm formation was detected utilizing the real time reverse transcription-polymerase chain reaction (RT-PCR) [17]. Therefore, most of the examples found in the literature make use of the mixed-ligand methodology to generate complexes or coordination polymers which include the muc ligand. Besides its interesting molecular length and diene functionality, muc dianion has two carboxylate groups which form an angle of  $120^\circ$  with an axle of the stiff diene part, thus, in the assembly of metal binding sites, syn-anti bridges are expected to form multi-dimensional frameworks. On the other hand, 2,2'-bipyridine derivatives, such as dmb, are interesting bi-dentate ligands, which are mainly used as coordination-sites blocking ligands for getting 1D or 2D coordination arrays; but also, they are very useful as crystalline structures-stabilizing compounds, via intermolecular interactions, in diverse coordination complexes and polymers. In addition, these types of ancillary ligands can influence sometimes luminescent characteristics of metal complexes.

Here, we report the synthesis, crystal structure and magnetic properties of dinuclear Co(II) muconate complex **1**, which shows a distorted-trigonal prismatic coordination sphere, that includes innocent and aqua ligands, as well as hydrogen-bonding 2D supramolecular array.

## Experimental

### Materials and Measurements

All chemicals were of analytical grade, purchased commercially (Aldrich) and used without further purification. Synthesis was carried out under aerobic and ambient conditions. Elemental analyses for C, H, N were obtained by standard methods using a Vario Micro-Cube analyzer. IR spectra of the complexes were determined in a FT-IR Shimadzu spectrophotometer, IR Prestige-21, from 4000 to  $500\text{ cm}^{-1}$ . Magnetic characteristics of **1** were determined in a MPMS

Quantum Design magnetometer with measurements performed at zero field cooling (ZFC) and field cooling (FC) from 2 to 300 K and decreasing. The applied magnetic field was 1000 Oe, and the total diamagnetic corrections were estimated using Pascal's constants as  $-250 \times 10^{-6} \text{ cm}^3 \text{ mol}^{-1}$ .

## Synthesis of **1**

A solution of sodium hydroxide (0.5 mmol) was added to a methanol–water 50:50 solution of *trans, trans*-muconic acid (0.25 mmol) while stirring for five minutes, then a methanol solution of 5,5'-dimethyl-2,2'-bipyridine (0.25 mmol) was poured while stirring. After five minutes, the ligands solution was added to a  $\text{Co}(\text{NO}_3)_2 \cdot 6\text{H}_2\text{O}$  (0.25 mmol) aqueous solution; a red colored solution was obtained. After eight days of slow evaporation of solvents, deep-red, small, prism-shape crystals were obtained, and then filtered, washed with a 50:50 deionized water–methanol solution and air-dried. Yield: 51.09% based on muc ligand.  $\text{C}_{36}\text{H}_{40}\text{Co}_2\text{N}_4\text{O}_{12}$ : calcd. C, 51.56%; H, 4.81%; N, 6.68%. Found: C, 51.16%; H, 4.90%; N, 6.66%. IR (ATR,  $\text{cm}^{-1}$ ): 3309 (w, br), 3059 (w, br), 2794 (w, br), 2383 (w, br), 1714 (sh), 1623 (w, sh), 1531 (s), 1520 (m), 1512 (m), 1504 (m, sh), 1477 (m, sh), 1404 (s, sh), 1370 (m, sh), 1319 (m, sh), 1289 (m, sh), 1250 (m, sh), 1234 (w), 1190 (w), 1162 (w), 1050 (w, sh), 1011 (m, sh), 964 (m, sh), 870 (m, sh), 832 (s, sh), 813 (m), 748 (m), 734 (s, sh), 693 (m, sh), 654 (m, sh), 646 (m), 572 (s, sh), 563 (m, sh) (Fig. S1).

## Crystal Structure Determination

X-ray diffraction data were collected on a Bruker SMART APEX DUO CCD diffractometer  $\text{Mo K}\alpha$  ( $\lambda = 0.71073 \text{ \AA}$ ) at 100(2) K. The crystal was coated with hydrocarbon oil, picked up with a nylon loop, and immediately mounted in the cold nitrogen stream ( $-173 \text{ }^\circ\text{C}$ ) of the diffractometer. Frames were collected by omega scans, integrated using SAINT program, and semiempirical absorption correction (SADABS) [18]. The structure was solved by direct methods (SHELXT) [19] and refined by the full-matrix least-squares on  $F^2$  with SHELXL-97 [20] using the SHELXLE GUI [21]. Weighted R factor and all goodness of fit indicator are based on  $F^2$ . All non-hydrogen atoms were refined anisotropically. Hydrogen atoms from C–H bonds were placed in idealized geometrical positions and refined with Uiso tied to the parent atom with the riding model, the hydrogen atoms of water molecules were found in the residual electron density map and fixed at standard distances (0.84  $\text{\AA}$ ) using DFIX instructions. A molecule of solvent (methanol) was found in the asymmetric unit with partial occupancy (31%),

**Table 1** Crystal data and structure refinement parameters for **1**

Empirical formula	$\text{C}_{36.30}\text{H}_{41.25}\text{Co}_2\text{N}_4\text{O}_{12.31}$
Formula weight	848.40
Temperature (K)	100(2)
Wavelength ( $\text{\AA}$ )	0.71073
Crystal system	Monoclinic
Space group	C2/c
$a$ ( $\text{\AA}$ )	36.2244(11)
$b$ ( $\text{\AA}$ )	6.2446(2)
$c$ ( $\text{\AA}$ )	17.1488(5)
$\alpha$ ( $^\circ$ )	90
$\beta$ ( $^\circ$ )	101.4118(6)
$\gamma$ ( $^\circ$ )	90
Volume ( $\text{\AA}^3$ )	3802.5(2)
$Z$	4
$D_{\text{calc}}$ ( $\text{mg}/\text{m}^3$ )	1.482
Absorption coefficient ( $\text{mm}^{-1}$ )	0.941
$F(000)$	1758
Crystal size ( $\text{mm}^3$ )	$0.428 \times 0.383 \times 0.162$
Theta range for data collection ( $^\circ$ )	2.423 to 27.433
Index ranges	$-46 \leq h \leq 46, -8 \leq k \leq 8,$ $-22 \leq l \leq 22$
Reflections collected	22,474
Independent reflections	4337 [R(int)=0.0384]
Refinement method	Full-matrix least-squares on $F^2$
Data/restraints/parameters	4337/114/311
Goodness-of-fit on $F^2$	1.043
Final R indices [ $I > 2\sigma(I)$ ]	$R1 = 0.0275, wR2 = 0.0671$
R indices (all data)	$R1 = 0.0311, wR2 = 0.0688$
Largest diff. peak and hole ( $e \text{ \AA}^{-3}$ )	0.369 and $-0.304$

the occupancy was refined using a free variable. The disordered ligand moiety in both compounds were refined using geometry (SADI, DFIX, SAME, FLAT) and Uij restraints (SIMU, RIGU, SADI, EADP) using free variable for occupancy implemented in SHELXL<sup>3</sup>. The occupancy ratio for majority position and second position was 84/16.

The crystallographic data and refinement details for **1** are summarized in Table 1. Selected bond distances and bond angles are listed in Table 2.

## Results and Discussion

### Synthesis

Synthesis of **1** was accomplished at ambient conditions by mixing  $\text{Co}(\text{NO}_3)_2 \cdot 6\text{H}_2\text{O}$  with the muc and dmb ligands in a water–methanol solution, yielding dark-red crystals of **1**,

**Table 2** Selected bond distances (Å), angles (°) and hydrogen bonding for **1**

Bond length (Å)				
Co(1)–O(4)	2.0385(12)	Co(1)–N(2)	2.1418(13)	
Co(1)–O(3)	2.0622(11)	Co(1)–O(2)	2.2936(11)	
Co(1)–O(1)	2.0991(11)			
Co(1)–N(1)	2.1061(13)			
Angles (°)				
O(4)–Co(1)–O(3)	86.77(5)	O(1)–Co(1)–N(2)	89.71(4)	
O(4)–Co(1)–O(1)	92.66(5)	N(1)–Co(1)–N(2)	76.83(5)	
O(3)–Co(1)–O(1)	102.04(5)	O(4)–Co(1)–O(2)	149.20(4)	
O(4)–Co(1)–N(1)	125.53(5)	O(3)–Co(1)–O(2)	85.94(4)	
O(3)–Co(1)–N(1)	96.64(5)	O(1)–Co(1)–O(2)	59.87(4)	
O(1)–Co(1)–N(1)	138.34(5)	N(1)–Co(1)–O(2)	85.06(4)	
O(4)–Co(1)–N(2)	88.46(5)	N(2)–Co(1)–O(2)	103.87(4)	
O(3)–Co(1)–N(2)	167.50(5)			
D–H $\cdots$ A	d(D–H)	d(H $\cdots$ A)	d(D $\cdots$ A)	<(DHA)
O(3)–H(3B) $\cdots$ O(6) <sup>#3</sup>	0.77(2)	2.03(3)	2.798(6)	178(2)
O(3)–H(3B) $\cdots$ O(6A) <sup>#3</sup>	0.77(2)	2.08(4)	2.85(3)	177(3)
O(3)–H(3A) $\cdots$ O(5) <sup>#4</sup>	0.87(2)	1.73(3)	2.592(2)	173(2)
O(3)–H(3A) $\cdots$ O(5A) <sup>#4</sup>	0.87(2)	1.78(3)	2.628(12)	166(2)
O(4)–H(4B) $\cdots$ O(6) <sup>#4</sup>	0.84(3)	1.78(3)	2.618(11)	175(3)
O(4)–H(4B) $\cdots$ O(6A) <sup>#4</sup>	0.84(3)	1.71(6)	2.56(6)	177(3)
O(4)–H(4A) $\cdots$ O(2) <sup>#5</sup>	0.79(2)	1.99(3)	2.7741(16)	172(2)

Symmetry transformations used to generate equivalent atoms:

<sup>#1</sup> –  $x + 1/2, -y + 5/2, -z$

<sup>#2</sup> –  $x + 1, -y + 2, -z + 1$

<sup>#3</sup>  $x, -y + 2, z - 1/2$

<sup>#4</sup>  $x, -y + 1, z - 1/2$

<sup>#5</sup>  $x, y - 1, z$

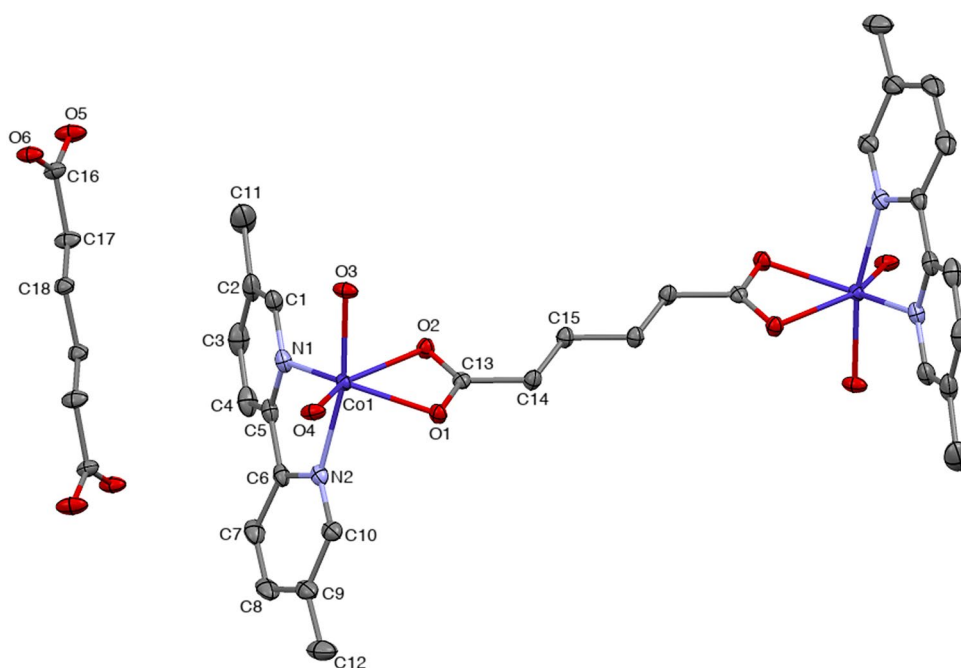
which structure was determined by elemental analysis, IR spectroscopy and single crystal X-ray diffraction studies.

### Crystal Structure of **1**

Complex **1** crystallizes in a monoclinic system with  $C2/c$  space group. The two Co(II) metals in the cation of complex **1** are hexa-coordinated with a  $N_2O_4$  distorted trigonal prismatic coordination environment (Fig. 1), coming from one bridging muc ligand, one dmb ligand and two coordinated water molecules. The metal to nitrogen distances are 2.1061(13) and 2.1418(13) Å, for N1 and N2, respectively. The metal to oxygen distances for the muc ligand are 2.0991(11) and 2.2936(11) Å, for O1 and O2, respectively. The M–O bonds for the coordinated water molecules are 2.0622(11) and 2.0385(12) Å for O3 and O4, respectively. The bite angle of the muc ligand is 59.87°, while the dmb ligand has a bite angle of 76.83°. These values are similar

to those obtained for other related Co(II) compounds [6, 22, 23], and also comparable to those values obtained in a Mn(II)-muconate 1D polymer having also distorted trigonal prismatic coordination geometry [7]. Thus, when the bite angle of a bidentate ligand tends to be small, such as in the muc ligand, the probability of obtaining hexa-coordinated complexes with a geometry closer to trigonal prismatic is higher. For **1**, the lengths of the triangular sides, in the distorted trigonal prismatic coordination geometry are in the range 2.917–2.993 Å for the triangle O1–N2–O4 and 2.974(2)–3.113(2) Å for the triangle O2–N1–O3, all angles belonging to these two prismatic triangles are in the range 56.12–65.49°. Two muc oxygen atoms (O1 and O2) and two oxygen atoms (O3 and O4), from the aqua ligands, form an irregular trapezoid, the sides of which are in the range of 2.199(3)–2.993(2) Å. The other two faces of the prism are also trapezoids involving the two oxygen atoms of the muc ligand and the two oxygen atoms of the aqua ligands, which

**Fig. 1** Molecular structure of **1** (ellipsoids shown at 60% probability). Hydrogens and methanol solvent molecule are omitted for clarity



are linked by the two nitrogen atoms of the dmb ligand, respectively (Fig. 2a). Both faces have an O–O distance of 2.199(3) and 2.817(2) Å, a N–O distance in the range 2.917(2)–3.113(2) Å, and of 2.640(2) Å for the N1–N2 side. Thus, the planes defined by O3–N1–O5 and O1–N2–O4 make an angle of 24.09° (Bailar angle). The torsion angles of the centroids of the triangular faces and each of the corners of the distorted prism (i.e., Ct1–N1–N2–Ct2) are 25.37, 27.64 and 29.13°, respectively. Regarding hexa-coordinated complexes, it is considered that if the Bailar twist angle is lower than 30° the coordination geometry approaches to a trigonal prism rather than to an octahedral one [3]. Furthermore, the counterion of complex **1** consists of a muc molecule, which is embedded in the crystalline structure of this compound. This type of dicarboxylate counterions are not common in coordination chemistry, particularly for dinuclear complexes, although there are some examples reported [24, 25]. As mentioned before, methanol solvent molecules were identified in the crystallography study of **1**. These solvent molecules were found trapped into the crystalline structure, as can be observed in Fig. 2b, but no further supramolecular interactions were observed. A TGA study of **1** demonstrated that methanol molecules were only inserted in the crystalline structure since they were lost at approximately 110 °C (Fig. S3).

Compound **1** generates a 2D supramolecular structure throughout hydrogen bonding (Fig. 3). These interactions can be observed in Fig. 3a, where the main hydrogen bonds are formed by the O–H moiety (O3 and O4) of the

aqua ligands with each of the oxygen atoms (O5 and O6) of the muc counter anion. Moreover, the aqua ligand (O4) forms another hydrogen bond with one oxygen atom (O2) of the muc ligand generating the extended 2D supramolecular array (Fig. 3b). This hydrogen bonding performed by the aqua ligands in **1**, seems to be the key structural component that, besides allowing the formation of a 2D supramolecular structure, promotes the generation of a unique distorted-trigonal prismatic (metaprism) coordination sphere around the Co(II) ions. Thus, complex **1** can be added to the few examples [6, 7, 26, 27] where the preference for a distorted-trigonal prismatic, over the typical octahedral coordination geometry, can be caused by supramolecular interactions, particularly, hydrogen bonding.

### Magnetic Properties of **1**

The plot of magnetic susceptibility ( $\chi$ ) (cm<sup>3</sup>/mol) vs. temperature for **1** is shown in Fig. 4a; and, as can be observed in Fig. 4b, the inverse magnetic susceptibility ( $\chi^{-1}$ ) vs. temperature plot was fitted to the Curie–Weiss model. From the Curie–Weiss model data fitting the Curie constant was determined to be 6.18 cm<sup>3</sup> K/mol. The Curie–Weiss temperature was determined to be  $\theta_{(C-W)} = -14.4$  K, indicative of an antiferromagnetic ordering. As expected, the low temperature decreasing of  $\chi^{-1}$  could be caused by weak intermolecular antiferromagnetic exchange because zero-field splitting of the  $^4T_{1g}$  ground state [28]. Often, the effects of spin–orbit coupling appear in combination with the impacts

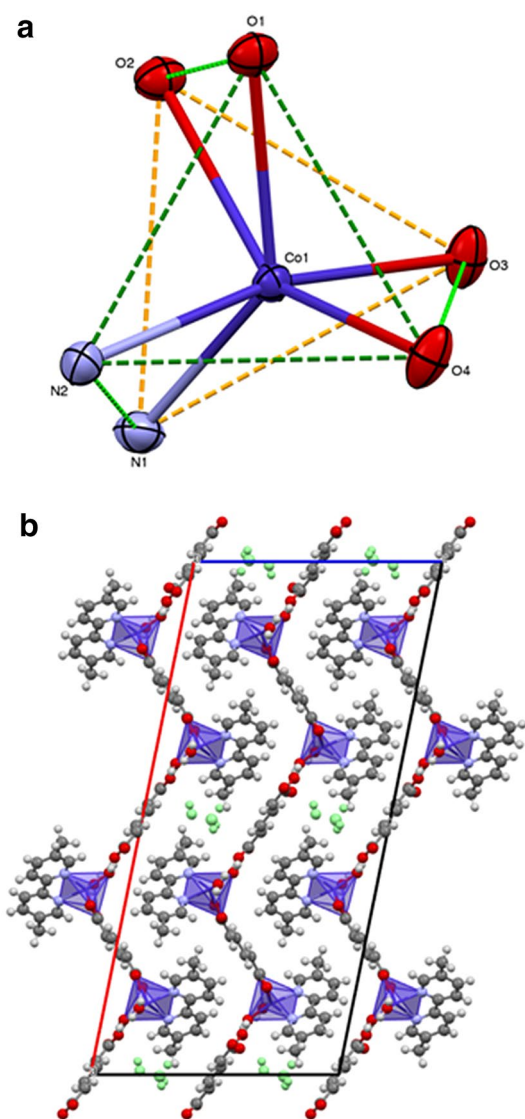


**Fig. 2** Co(II) coordination sphere in **1** showing the distorted-trigonal prismatic geometry (a). Unit cell of **1**. Methanol molecules shown in light green color (b) (ellipsoids shown at 60% probability)

of a symmetry-lowering structural distortion, as occurs in complex **1**, which structure deviates from the  $O_h$  symmetry [29]. From Curie–Weiss model a  $\mu_{\text{eff}} = 7.0 \mu_B$  is calculated, which is much higher than the expected spin-only value of  $3.87 \mu_B$  corresponding to three unpaired electrons for high-spin  $d^7\text{-Co}^{2+}$ ; however, the obtained value agrees with  $\mu_{\text{eff}} = 6.63 \mu_B$  corresponding to  $J = 9/2$ , indicating that the orbital moment is not quenched. This value is in agreement with the reported values reported in literature for dinuclear high-spin Co(II) complexes and also confirms a  $J = 9/2$  spin state [30]. Nonetheless, to fit the Curie–Weiss model to the  $\chi$  vs.  $T$  plot for the dinuclear complex **1** was complicated,

specifically below 30 K (Fig. 4a). So, believing that in the low-temperature region the spin–orbit coupling is promoted in this system, the magnetic exchange interactions and the spin–orbit coupling for complex **1** were also estimated based on the Rueff phenomenological equation  $\chi T = A \exp(-E_1/kT) + B \exp(-E_2/kT)$ , where  $A + B$  is equal to the Curie constant and  $E_1$  and  $E_2$  are the “activation energies” of the spin–orbit coupling and the antiferromagnetic interaction, respectively [31]. As shown in Fig. 4a, for the  $\chi$  vs.  $T$  plot, Rueff model follows very well the experimental data, even at the lowest temperature analyzed. The best parameters obtained with this method, after least-squares fitting, are  $A + B = 6.19 \text{ cm}^3 \cdot \text{K} \cdot \text{mol}^{-1}$ , which practically matches the value obtained from the fitting of Curie–Weiss model. The effect of the spin–orbit coupling  $E_1/k = 33.42 \text{ K}$  ( $E_1 = 23.22 \text{ cm}^{-1}$ ) is lower than values reported for other Co(II) systems, which are around  $50 \text{ cm}^{-1}$  [32, 33]. The positive and very low value of the activation energy  $E_2/k = 0.047 \text{ K}$  ( $E_2 = 0.032 \text{ cm}^{-1}$ ) validates both conditions, that antiferromagnetic exchanges are effective in complex **1** and that these interactions are weak. It could be assumed that the main magnetic exchange pathway could be the hydrogen bonding interactions involving the coordinated water molecules (O3 and O4) and the oxygen atom (O2) in the carboxylate of muc ligand, as well as the oxygen atom (O6) of one of the carboxylate of muc counter anion of **1** (Fig. 3a); in this supramolecular array, Co(II) centers are at a distance of approximately  $6.2 \text{ \AA}$  (Fig. S2).

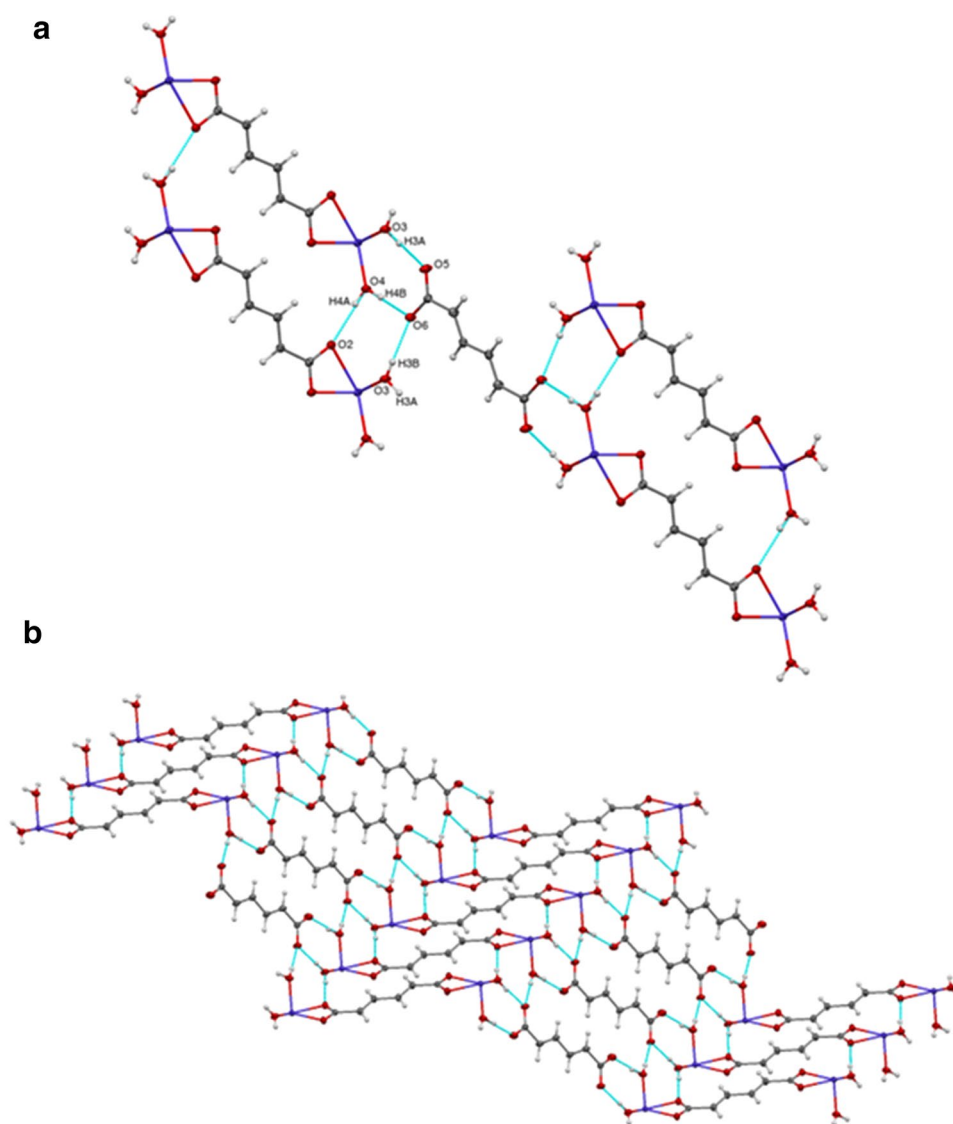
## Conclusion

Complex **1** represents the first example of a dinuclear Co(II) muconate-bridged complex, exhibiting a distorted-trigonal prismatic coordination geometry having, the so-called, “innocent” bidentate ligands and, specially, aqua ligands in its coordination sphere. Magnetic properties of **1** follows well the Curie–Weiss law and the Rueff model, with a  $\theta = -14.4 \text{ K}$  and  $E_2 = 0.032 \text{ cm}^{-1}$ , respectively, demonstrating thus the existence of weak antiferromagnetic interactions. Coordination geometry and magnetic properties of metaprisim **1** can be attributed predominantly to its 2D supramolecular array in the crystalline state.

## Supplementary Data

CCDC-2082430 contains supplementary crystallographic data for **1**. These data can be obtained free of charge via <http://www.ccdc.cam.ac.uk/conts/retrieving/html>, or from

**Fig. 3** Molecular structure of **1** showing main hydrogen bonding interactions (**a**) and 2D supramolecular array (**b**) (ellipsoids shown at 60% probability); dmb ligand is omitted for clarity



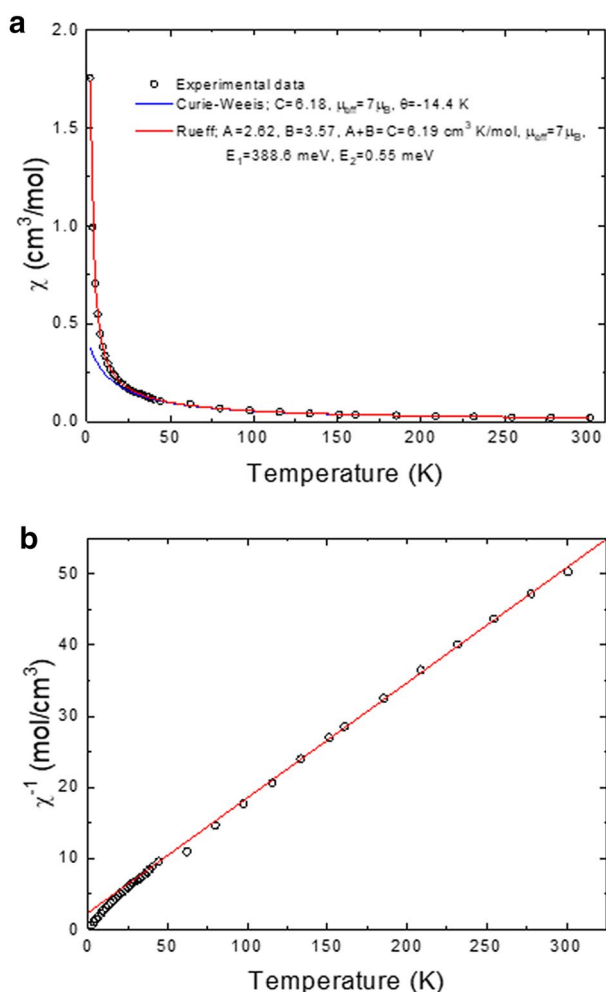


**Fig. 4**  $\chi$  vs.  $T$  (a) and  $\chi^{-1}$  vs.  $T$  (b) plots for 1

Cambridge Crystallographic Data Center (CCDC), 12 Union Road, Cambridge CB2 1EZ, UK [Fax: (+44) 1223-336-033; Email: deposit@cdc.cam.ac.uk].

**Supplementary Information** The online version contains supplementary material available at <https://doi.org/10.1007/s10870-021-00907-z>.

**Acknowledgements** The authors are thankful to M. en C. Alejandra Nuñez Pineda and L. I. A. María Citlalit Martínez Soto (CCIQS UAEM-UNAM) for elemental analysis and computing assistance, respectively. Funding for this work was provided by Universidad Autónoma del Estado de México. JJG thanks CONACyT for PhD scholarship (701384). R. Escudero acknowledges DGAPA-UNAM, project 1T100217. Authors thank M. C. Ana Bobadilla for liquid He, Carlos Reyes Damian for technical support, A. López and A. Pompa-García for help with graphs and figures.

## Declarations

**Conflict of interest** The authors declare that they have no conflict of interest.

## References

- Voloshin YZ, Lebedev AY, Novikov VV, Dolganov AV, Vologzhanina AV, Lebed EG, Pavlov AA, Starikova ZA, Buzin MI, Bubnov YN (2013) *Inorg Chim Acta* 399:67
- Cremades E, Echeverría J, Alvarez S (2010) *Chem Eur J* 16:10380–10396
- Santiago A (2015) *Chem Rev* 115:13447–13483
- Sreerama SG, Pal S (2001) *Inorg Chem Commun* 4:656–660
- Friese JC, Krol A, Puke C, Kirschbaum K, Giolando DM (2000) *Inorg Chem* 39:1496–1500
- Téllez-López A, Jaramillo-García J, Martínez-Domínguez R, Morales-Luckie RA, Camacho-Lopez MA, Escudero R, Sánchez-Mendieta V (2015) *Polyhedron* 100:373–381
- Jaramillo-García J, Sánchez-Mendieta V, García-Orozco I, Morales-Luckie RA, Martínez-Otero D, Téllez-López A, Rosales-Vázquez LD, Escudero R, Morales F (2018) *Z Anorg Allg Chem* 664:19–22
- Girrane A, Pastor A, Galindo A, Alvarez E, Mealli C, Ienco A, Orlandini A, Rosa P, Caneschi A, Barra A-L, Sanz JF (2011) *Chem Eur J* 17:10600–10617
- Chen B, Jiang F, Han L, Wu B, Yuan D, Wu M, Hong M (2006) *Inorg Chem Commun* 9:371–374
- Mir MH, Kitagawa S, Vittal JJ (2008) *Inorg Chem* 47:7728–7733
- Mir MH, Vittal JJ (2013) *Inorg Chim Acta* 403:97–101
- Mir MH, Koh LL, Tan GK, Vittal JJ (2010) *Angew Chem* 122:400–403
- Cotton FA, Donahue JP, Murillo CA (2003) *J Am Chem Soc* 125:5436–5450
- Mukherjee PS, Das N, Kryshchenko YK, Arif AM, Stang PJ (2004) *J Am Chem Soc* 126:2464–2473
- Nagaraja CM, Ugale B (2018) *Polyhedron* 155:433–440
- Ahmed F, Roy S, Naskar K, Sinha C, Alam SM, Kundu S, Vittal JJ, Mir MH (2016) *Cryst Growth Des* 16(9):514–5519
- Fu D, Yang S, Lu J, Lian H, Qin K (2021). *J Clust Sci.* <https://doi.org/10.1007/s10876-021-01996-8>
- Bruker, S. A. D. A. B. S., & SAINT, S. (2007). Bruker AXS Inc. Madison, Wisconsin, USA.
- Sheldrick GM (2015) SHELXT—Integrated space-group and crystal-structure determination. *Acta Crystallogr Sect A* 71(1):3–8
- Sheldrick GM (2015) Crystal structure refinement with SHELXL. *Acta Crystallogr Sect A* 71(1):3–8
- Hübschle CB, Sheldrick GM, Dittrich B (2011) ShelXle: a Qt graphical user interface for SHELXL. *J Appl Crystallogr* 44(6):1281–1284
- Mihalciak J, Bertová P, Růžičková Z, Moncol J, Segla P, Boča R (2015) *Inorg Chem Commun* 56:62–64
- Sakiyama H, Ito R, Kumagai H, Inoue K, Sakamoto M, Nishida Y, Yamasaki M (2001) *Eur J Inorg Chem* 8:2027–2032
- Padmanabhan M, Joseph JC, Huang X, Li J (2008) *Mol J Struct* 885:36–44



25. Kim JC, Lough AJ, Park H, Kang YC (2006) *Inorg Chem Commun* 9:514–517
26. Van Gorkum R, Buda F, Kooijman H, Spek AL, Bouwman E, Reedijk J (2005) *Eur J Inorg Chem* 12:2255–2261
27. Schoedela A, Zaworotko MJ (2014) *Chem Sci* 5:1269–1282
28. Murrie M (2010) *Chem Soc Rev* 39:1986–1995
29. Kahn O (1993) *Molecular magnetism*. VCH Publishers, Hoboken, p 393
30. Narayanan J, Solano-Peralta A, Ugalde-Saldivar VM, Escudero R, Höpfl H, Sosa-Torres ME (2008) *Inorg Chim Acta* 361(9–10):2747–2758
31. Rabu P, Rueff JM, Huang ZL, Angelov S, Souletie J, Drillon M (2001) *Polyhedron* 20:1677
32. Rueff JM, Masciocchi N, Rabu P, Sironi A, Skoulios A (2001) *Eur J Inorg Chem* 2011(11):2843
33. Rueff JM, Masciocchi N, Rabu P, Sironi A, Skoulios A (2002) *Chem Eur J* 8:1813

**Publisher's Note** Springer Nature remains neutral with regard to jurisdictional claims in published maps and institutional affiliations.

## Authors and Affiliations

Jonathan Jaramillo-García<sup>1</sup> · Raúl A. Morales-Luckie<sup>2</sup> · Diego Martínez-Otero<sup>2</sup> · Víctor Sánchez-Mendieta<sup>2</sup>  · Roberto Escudero<sup>3</sup> · Francisco Morales<sup>3</sup>

✉ Víctor Sánchez-Mendieta  
vsanchezm@uaemex.mx

<sup>1</sup> Posgrado en Ciencia de Materiales, Facultad de Química, Universidad Autónoma del Estado de México, Paseo Colón y Paseo Toluca, 50120 Toluca, Estado de México, Mexico

<sup>2</sup> Centro Conjunto de Investigación en Química Sustentable, UAEM-UNAM, Carretera Toluca-Atlacomulco Km. 14.5, San Cayetano, 50200 Toluca, Estado de México, Mexico

<sup>3</sup> Instituto de Investigaciones en Materiales, Universidad Nacional Autónoma de México, Apartado Postal 70-360, 04510 Mexico, Mexico